New Results from LUX-ZEPLIN:
Beyond Spin-Independent WIMPs

Greg Rischbieter
Postdoctoral Associate, University of Michigan & University of Zürich
on behalf of the LUX-ZEPLIN Collaboration
Rencontres de Moriond, EW 2024

LZ (LUX-ZEPLIN) Collaboration,

38 Institutions → 250 scientists, engineers, and technical staff

@lzdarkmatter

https://lz.lbl.gov/

- Black Hills State University
- Brookhaven National Laboratory
- Brown University
- Center for Underground Physics
- Edinburgh University
- Fermi National Accelerator Lab.
- Imperial College London
- King's College London
- Lawrence Berkeley National Lab.
- Lawrence Livermore National Lab.
- LIP Coimbra
- Northwestern University
- Pennsylvania State University
- Royal Holloway University of London
- SLAC National Accelerator Lab.
- South Dakota School of Mines & Tech
- South Dakota Science & Technology Authority
- STFC Rutherford Appleton Lab.
- Texas A&M University
- University of Albany, SUNY
- University of Alabama
- University of Bristol
- University College London
- University of California Berkeley
- University of California Davis
- University of California Los Angeles
- University of California Santa Barbara
- University of Liverpool
- University of Maryland
- University of Massachusetts, Amherst
- University of Michigan
- University of Oxford
- University of Rochester
- University of Sheffield
- University of Sydney
- University of Texas at Austin
- University of Wisconsin, Madison
- University of Zürich

US Europe Asia Australia

FCT
Fundação para a Ciência e a Tecnologia
MINISTÉRIO DA EDUCAÇÃO E CIÊNCIA

UKRI Science and Technology Facilities Council

ibs Institute for Basic Science

Sanford Underground Research Facility
South Dakota Science and Technology Authority

Thanks to our sponsors and participating institutions!

WIMP Direct Detection with a Dual Phase TPC

- The Time Projection Chamber (TPC) allows for Reconstruction of the Number of Scatters, Interaction Position, and Energy
- Measures the Scintillation (S1) and Ionization (S2) response of LXe following an energy deposit
- LXe targets: 2.9 g/cc → Low-rate of penetration of ER backgrounds into the inner volume: "self-shielding"

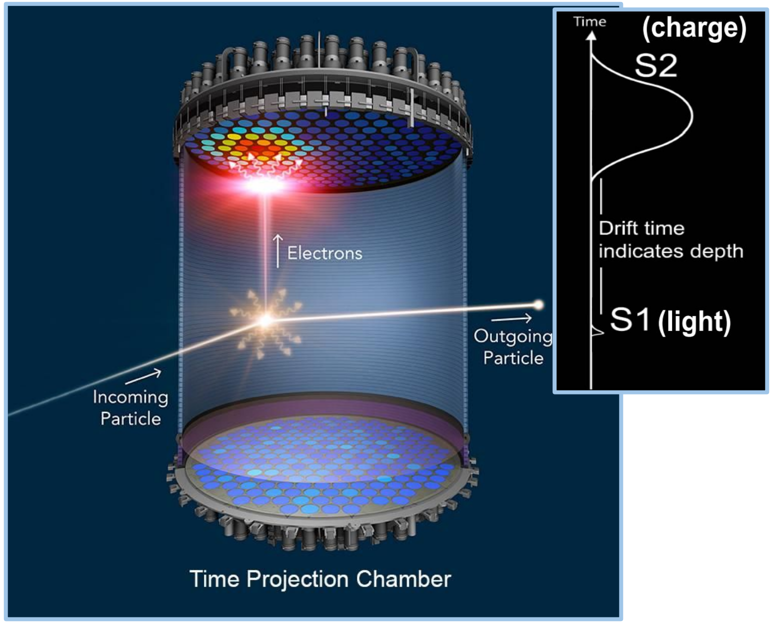

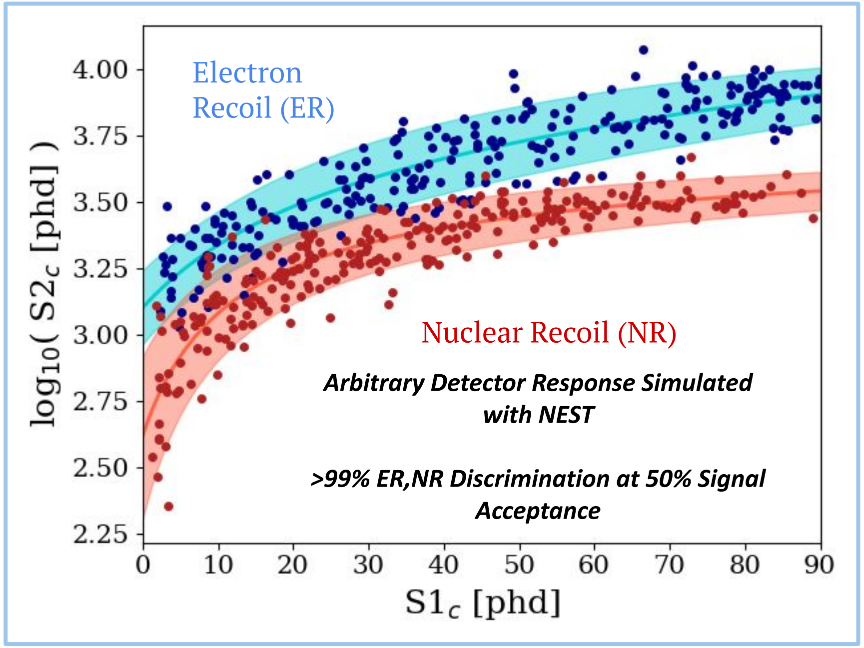

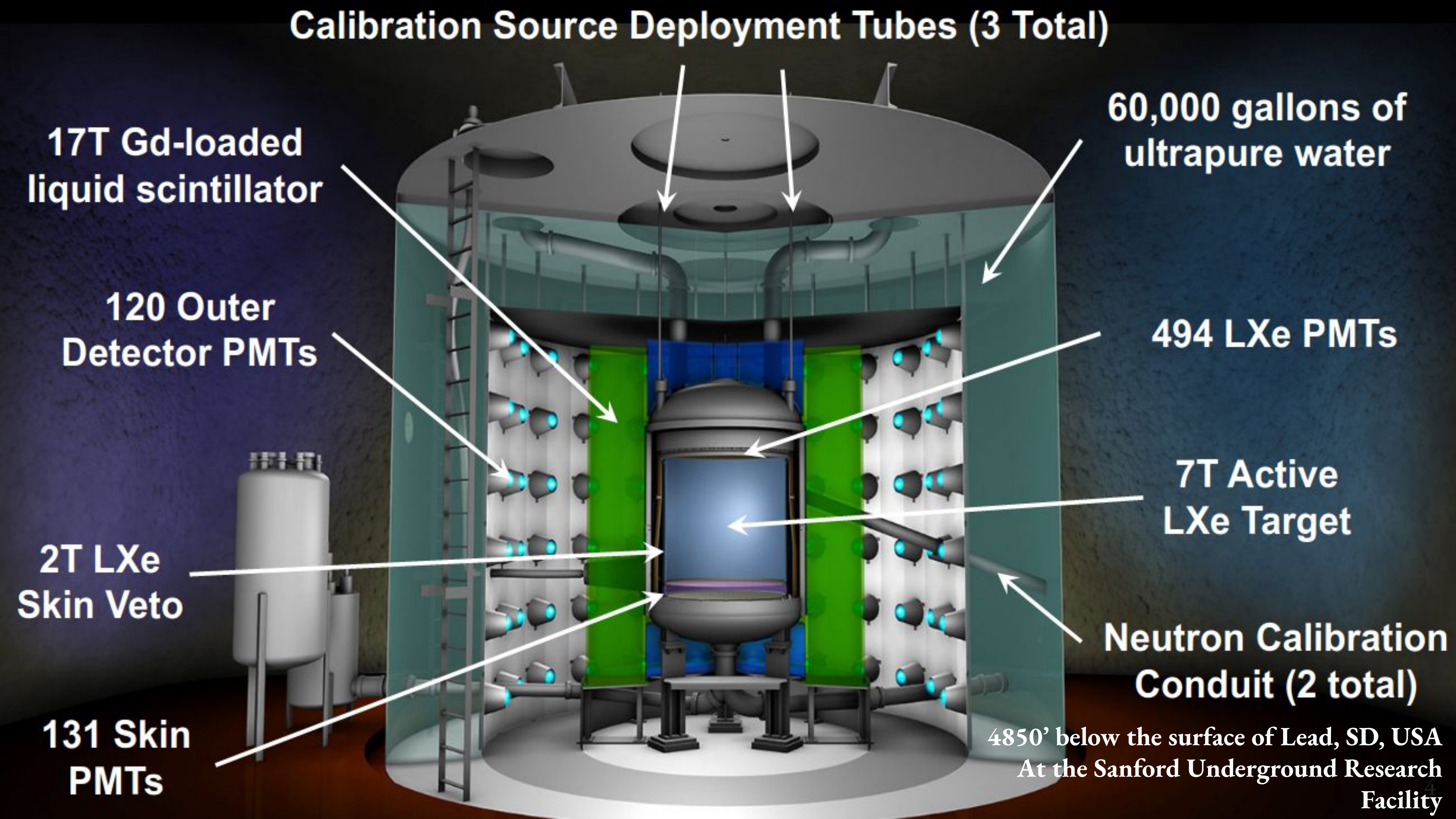
Calibration Source Deployment Tubes (3 Total)
17T Gd-loaded liquid scintillator
120 Outer Detector PMTs
2T LXe Skin Veto
131 Skin PMTs
60,000 gallons of ultrapure water
494 LXe PMTs
7T Active LXe Target
Neutron Calibration Conduit (2 total)
4850’ below the surface of Lead, SD, USA
At the Sanford Underground Research Facility

LZ's First Results: Recap and Overview

Detector Conditions

- Drift field: 193 V/cm
- Extraction field: 7.3 kV/cm

Dataset

- Data collected between Dec. 2021-May 2022
- 60 ± 1 live days
- 5.5 ± 0.2 tonne fiducial volume

Analysis

- ER Calibration (tritium)
- NR Calibration (D-D Fusion neutrons)
- Backgrounds well modeled (see Phys. Rev. D 108, 012010)
- Unbinned profile likelihood analysis in $\log_{10}$(S2c)-S1c space
- Results: Phys. Rev. Lett. 131, 041002

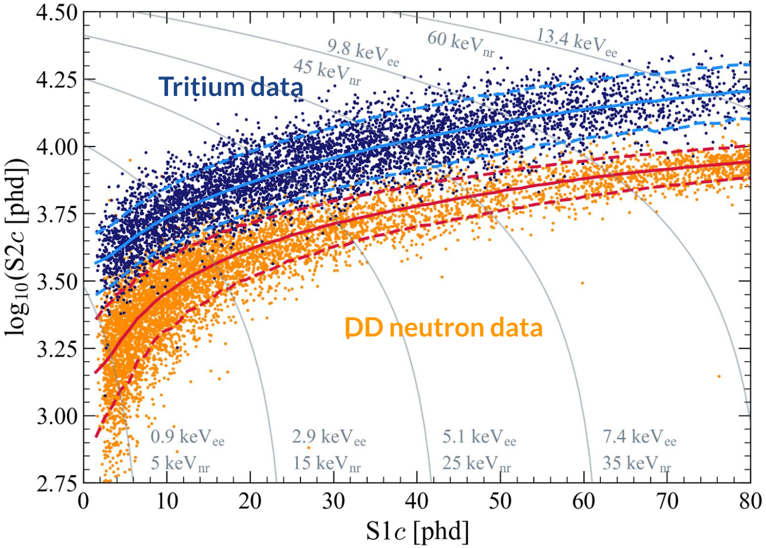

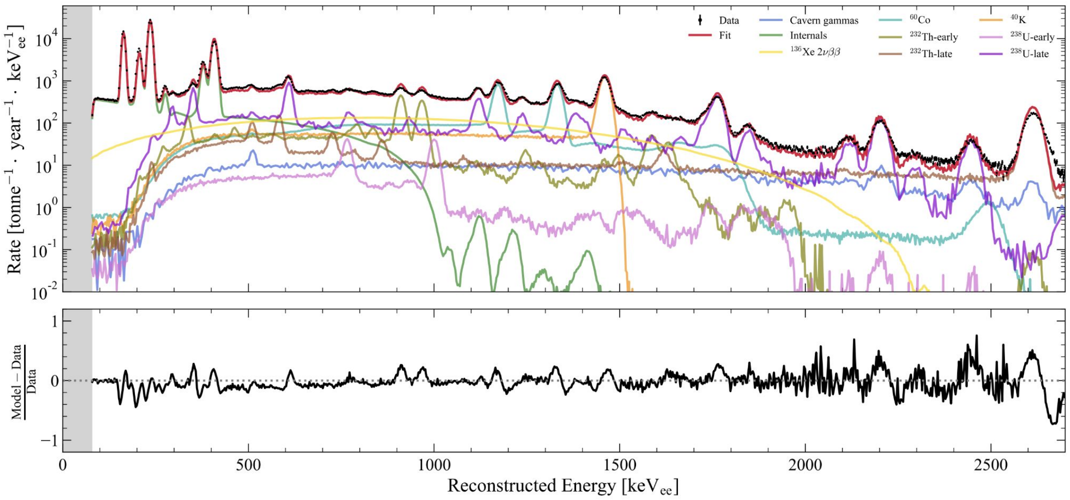

LZ's First Results: Recap and Overview

- 335 Events Observed
- Consistent with background-only hypothesis, using two-sided PLR analysis framework
- Most stringent cross-section limit at 36 GeV/c^2: 9.2×10^{-48} cm^2
  - Power-constrained at -1σ
- World-leading exclusion limit for masses above 9 GeV/c^2
- See M. Hernandez's talk from yesterday's VHEPU session for more details and results from our First Dataset

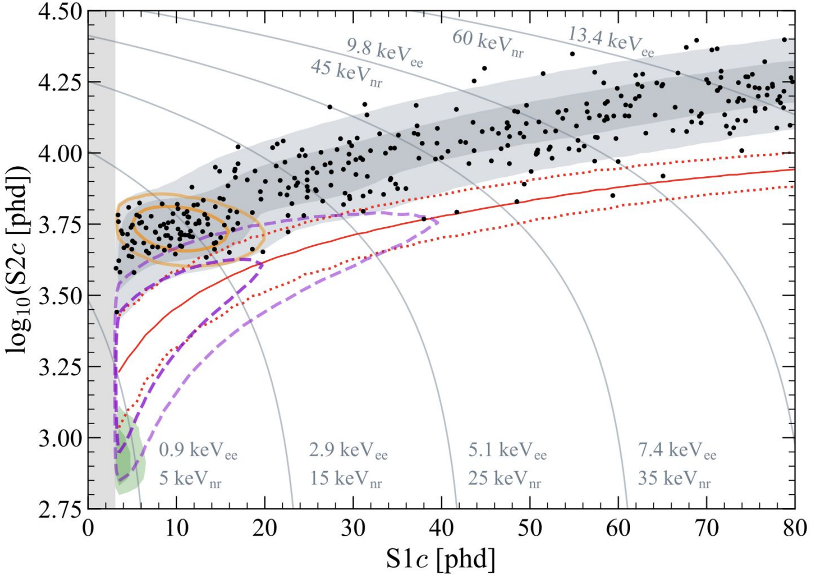

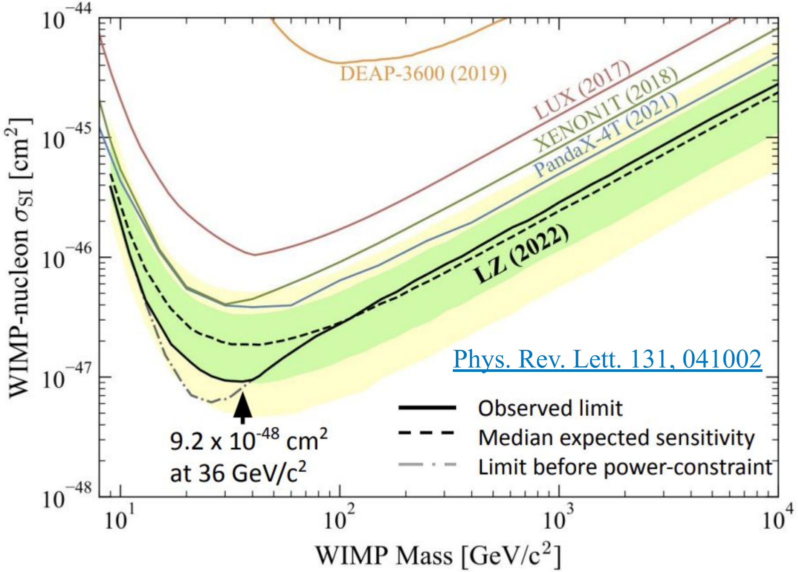

No WIMPs Observed… What's Next?

No WIMPs Observed… What's Next?

1. Collect More Data (ongoing)

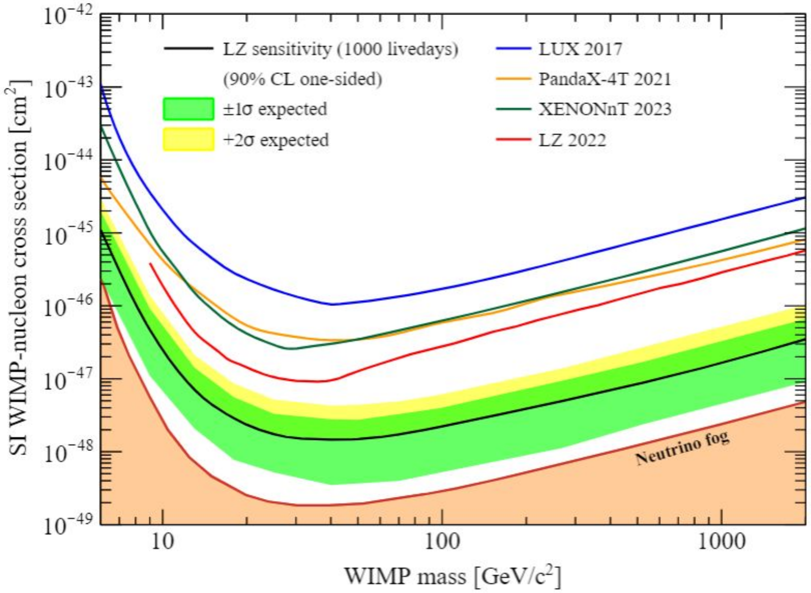

No WIMPs Observed… What's Next?

1. Collect More Data (ongoing)
2. Look in More Places!

Going Further: Operators in a Non-Relativistic Effective Field Theory

Phys. Rev. C 89, 065501 (2014)
JCAPO2 (2013)

- Spin Independent and Spin Dependent interactions rely on the assumption of a zero-momentum transfer. But what if there is some momentum dependency?
- Use an EFT where we treat the WIMP-nucleon elastic scattering as a four-field interaction

$$\mathcal{L}_{int} = \mathcal{O}\chi^{+}\chi^{-}N^{+}\mathrm{N}^{-}$$

- 4 Galilean-invariant, Hermitian quantities which describe the interaction

$$i\vec{q},\ \vec{S}_{\chi},\ \vec{S}_{N},\ \vec{v}^{\perp} \equiv \vec{v} + \frac{\vec{q}}{2\mu_N}$$

- Linear combinations up to second-order of momentum →15 operators which contribute to the interaction Lagrangian

$$\begin{aligned}
\mathcal{L}_{int} &= \sum_i c_i \mathcal{O}_i \\
&= c_1 + ic_3\vec{S}_N\cdot(\vec{q}\times\vec{v}^{\perp}) + c_4\vec{S}_{\chi}\cdot\vec{S}_N \\
&+ ic_5\vec{S}_{\chi}\cdot(\vec{q}\times\vec{v}^{\perp}) + c_6(\vec{S}_{\chi}\cdot\vec{q})(\vec{S}_N\cdot\vec{q}) \\
&+ c_7\vec{S}_N\cdot\vec{v}^{\perp} + c_8\vec{S}_{\chi}\cdot\vec{v}^{\perp} + ic_9\vec{S}_{\chi}\cdot(\vec{S}_N\times\vec{q}) \\
&+ c_{10}\vec{S}_N\cdot\vec{q} + ic_{11}\vec{S}_{\chi}\cdot\vec{q} + c_{12}\vec{S}_{\chi}\cdot(\vec{S}_N\times\vec{v}^{\perp}) \\
&+ ic_{13}(\vec{S}_{\chi}\cdot\vec{v}^{\perp})(\vec{S}_N\cdot\vec{q}) + ic_{14}(\vec{S}_{\chi}\cdot\vec{q})(\vec{S}_N\cdot\vec{v}^{\perp}) \\
&+ -c_{15}(\vec{S}_{\chi}\cdot\vec{q})\left((\vec{S}_N\times\vec{v}^{\perp})\cdot\vec{q}\right)
\end{aligned}$$

Recoil Rates from NREFT Operators

- Simplest case: assume no interference between operators: $c_i c_j = 0$ for i≠j
- Typical SI WIMP Search: 0-50 keV
  - Poor search window for NREFT Interactions!
- Shaded regions are where detection threshold falls below 50% after final data selection criteria

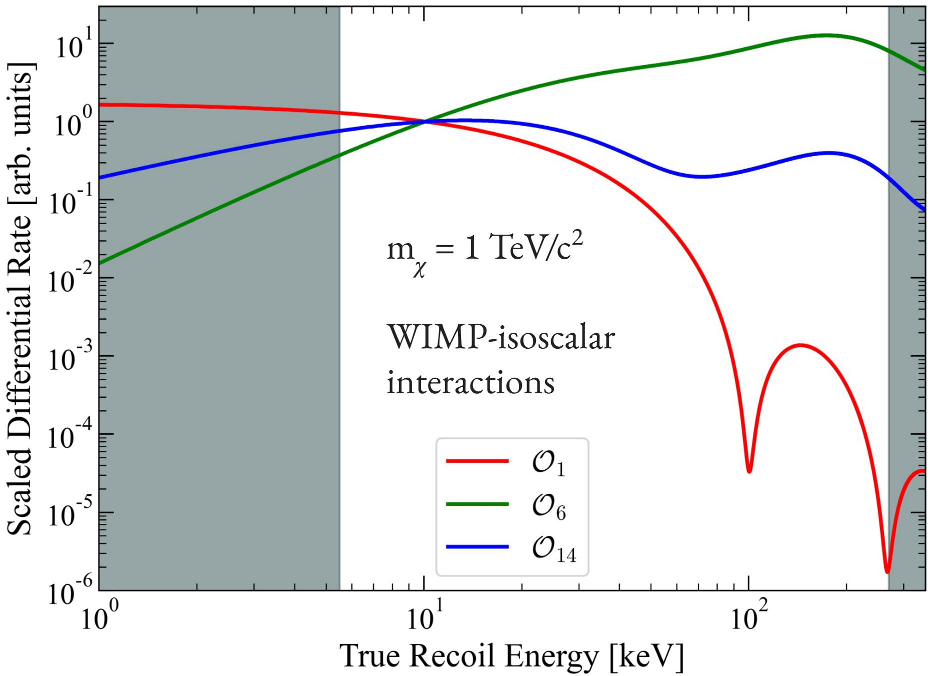

Differential rates in evts/kg/day/keV normalized at ~10 keV for shape visualization

Extending the Energy Window

- ER Response Model extended to higher energies with a ^{212}Pb calibration (injection of ^{220}Rn)
- NR Response Model extrapolated using NEST (github.com/NESTCollaboration/nest)
  - NR Uncertainty (pink) beyond D-D endpoint quantified by comparing NEST to *ex situ* datasets of AmBe neutrons (Phys. Rev. D **83**, 063501) and D-T fusion neutrons (Phys. Rev. D **106**, 052013)

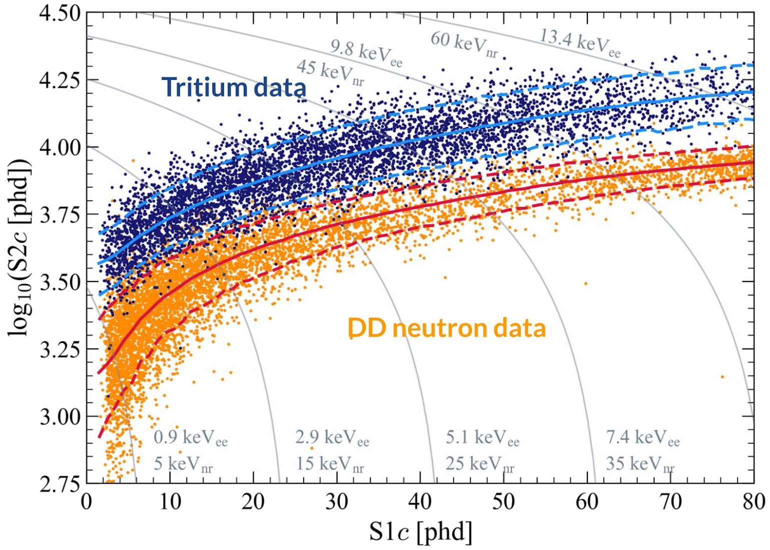

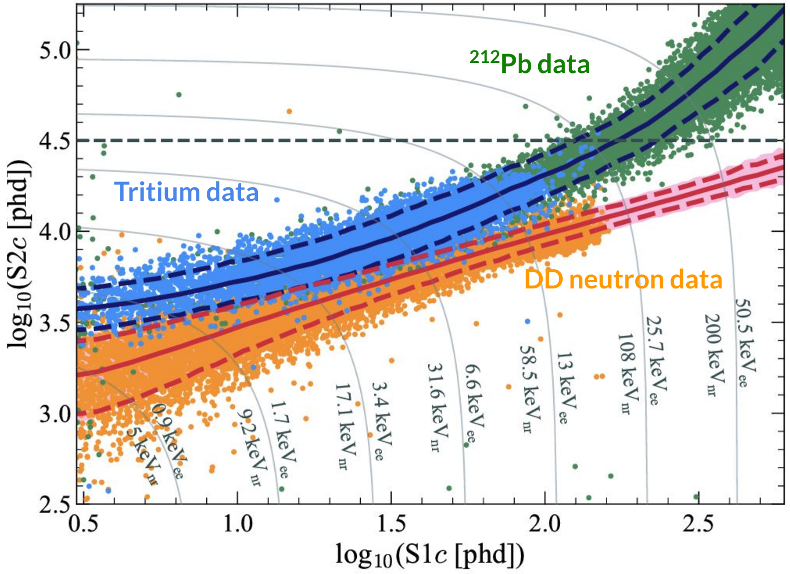

Assessing Newly Introduced Backgrounds

- Extending the search window introduces more backgrounds than in the Spin-Independent Search
  - Additional Xe decay contributions: ^{124}Xe, ^{136}Xe, and ^{127}Xe
  - Electron capture on ^{125}I
  - Increased rate of ERs from detector components (observed near the fiducial volume edges)
  - More Detector ER pathologies (due to things such as field non-uniformity and multiple scattering)

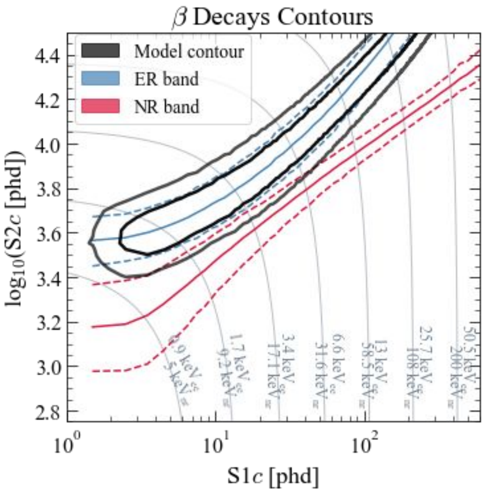

Source	Expected Events
Flat ER	517.4 ± 82.8
Detector ER	18.4 ± 9.2
ν ER	55.3 ± 5.5
^{124}Xe	8.2 ± 2.0
^{127}Xe	20.5 ± 1.8
^{136}Xe	55.1 ± 11.6
^{125}I	30.1 ± 15.6
^{8}B CEνNS	0.14 ± 0.01
Accidentals	1.3 ± 0.3
Subtotal	706 ± 86
^{37}Ar	[0, 288]
Detector neutrons	$0.0^{+0.5}$

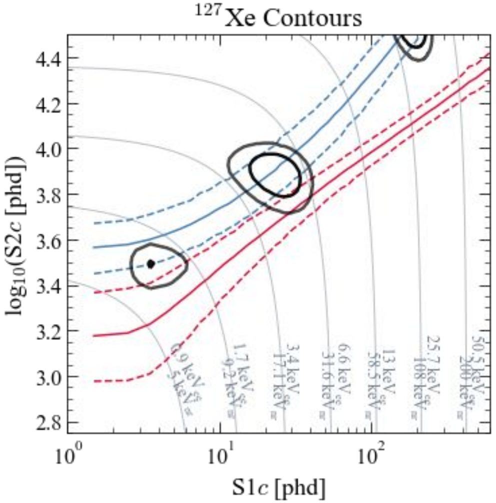

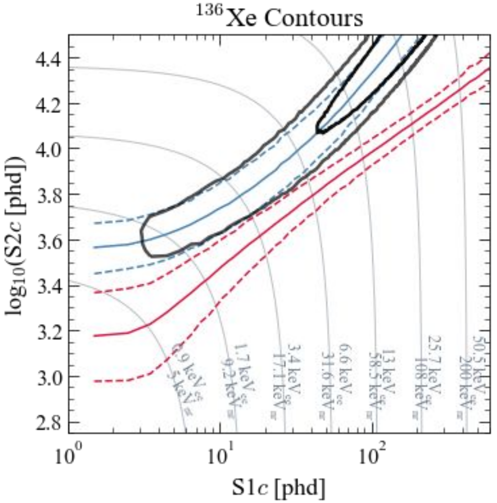

WIMP-like ER Pathologies: γ-X Events

- **γ-X Events**: Multiple S1-contributing scatters, one S2-contributing scatter
  - Can mimic a nuclear recoil
  - Custom simulation framework utilizing LZ geometry, field maps, and NEST response models to simulate γ propagation and yields for multiply-scattering events
- Boosted Decision Tree trained on simulated data and tested on calibration and side band datasets
  - Expected 1.6 ± 0.3 events below S1c = 600 phd → two were tagged and removed

↓ P, → T	SS	γ-X
SS	99.997 ± 0.005	0.4 ± 1.2
γ-X	0.003 ± 0.005	99.6 ± 1.2

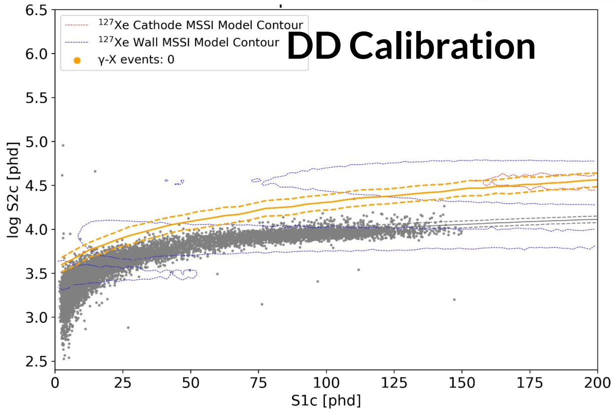

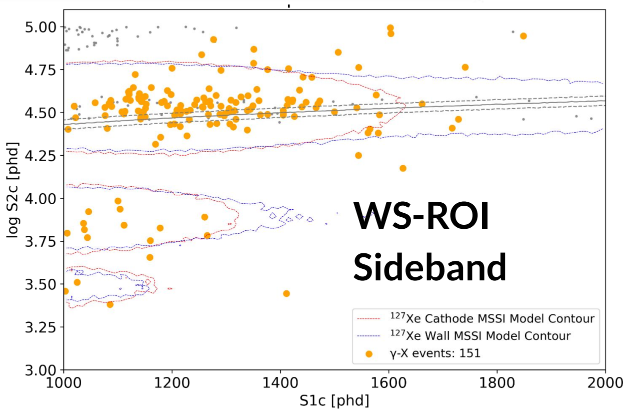

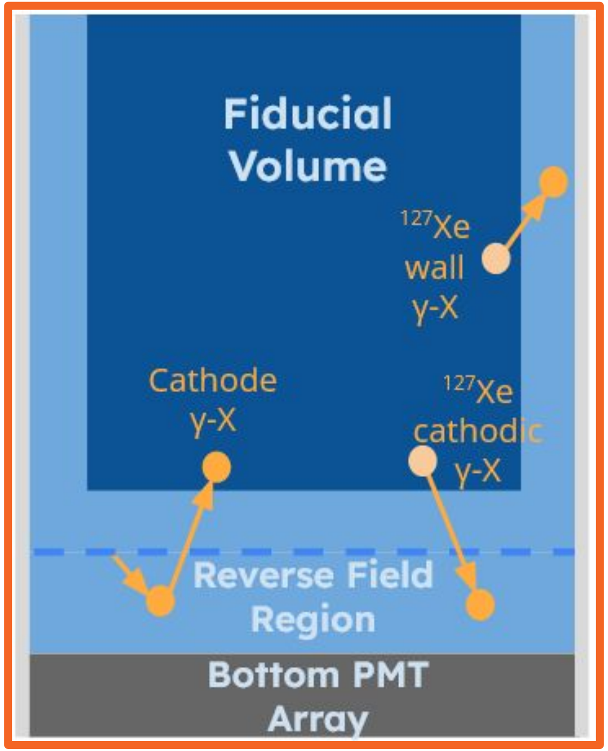

Observed Data

- 835 events after selection criteria and implementation of Skin and OD vetoes
- 3 < S1c [phd] < 600 $\log_{10}$(S2c) < 4.5
- Same 5.5 ± 0.2 tonne fiducial volume definition as the Spin-Independent WIMP search

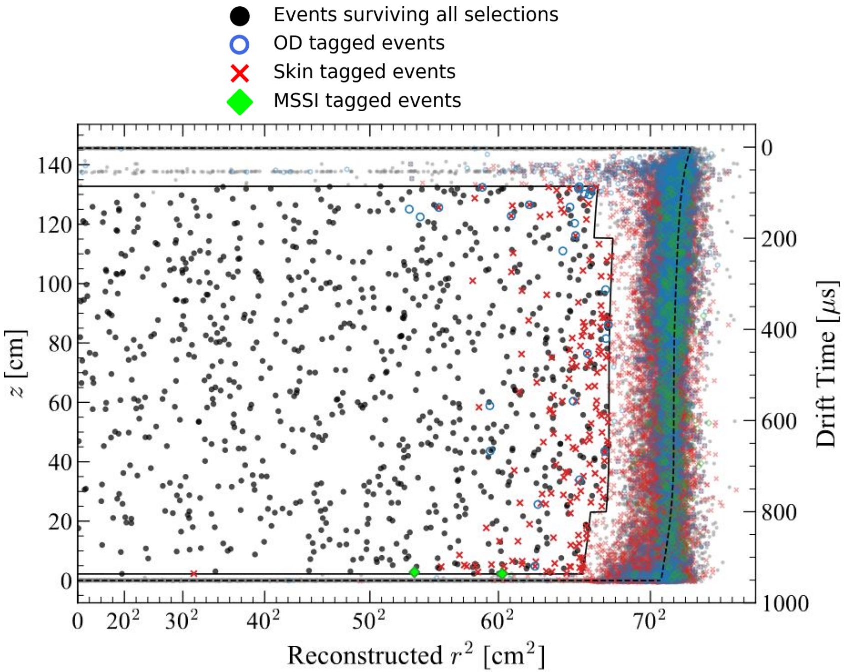

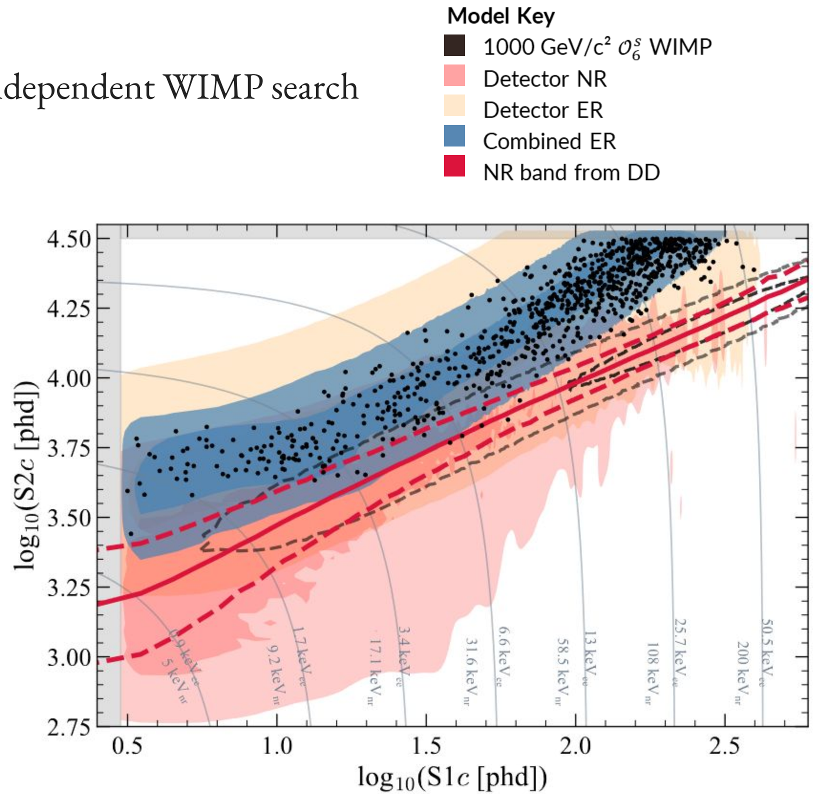

Results

- With our region of interest set and models prepared, we can test a range of models
  - Operators 1 through 15
  - Isoscalar and isovector couplings
  - Elastic and Inelastic WIMP recoils
- Consistent with the Background-Only Hypothesis
  - World-leading limits for each operator (except O_{13})

Elastic Scattering: O_1 (Similar to SI)

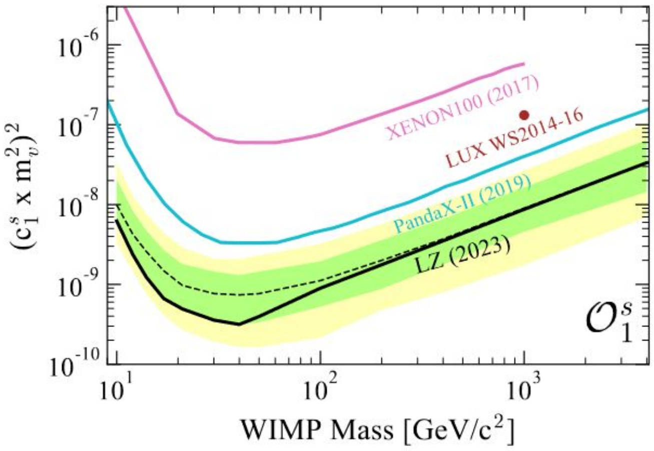

Elastic Scattering: O_6

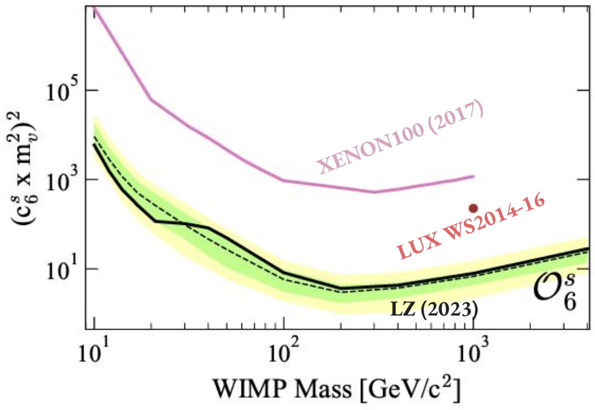

Inelastic Scattering: O_4
(Circles are LUX Results Phys. Rev. D 104, 062005)

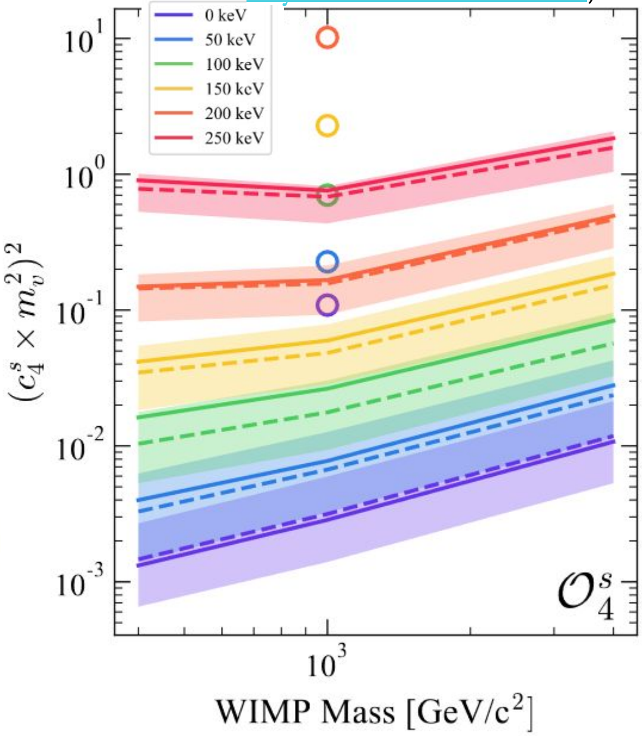

Operator Results at m_χ=1000 GeV/c^2

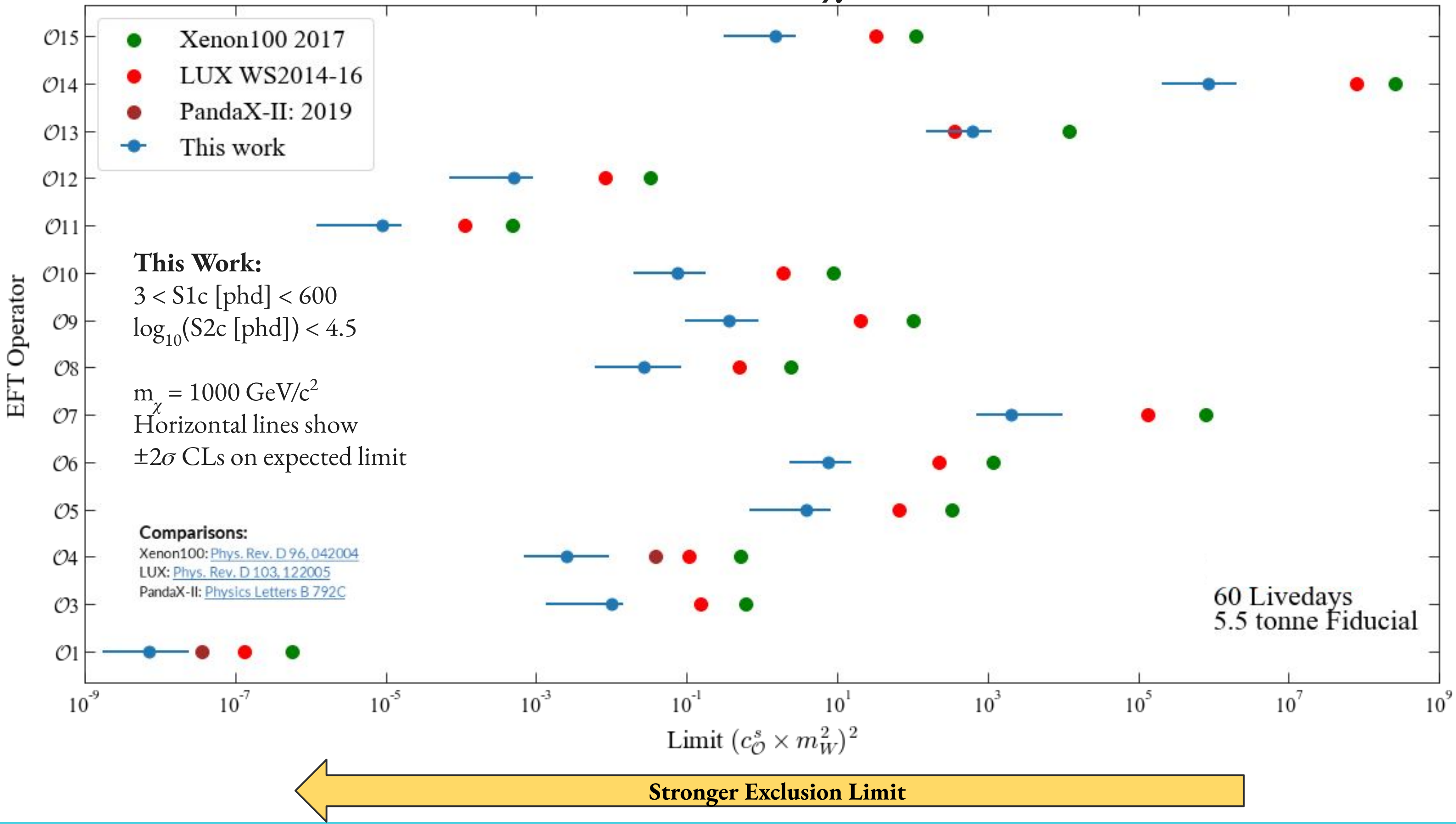

Summary

With its first science run, LZ has set world-leading limits for dozens of WIMP models

Backgrounds are well-understood and accurately modeled

Data collection ongoing! Stay tuned for more results!

Paper on arXiv:
arXiv:2312.02030

Accepted to Phys. Rev. D this week!

arXiv:2312.02030v2 [hep-ex] 26 Feb 2024

First Constraints on WIMP-Nucleon Effective Field Theory Couplings in an Extended Energy Region From LUX-ZEPLIN

J. Aalbers,[1,2] D.S. Akerib,[1,2] A.K. Al Musalhi,[3] F. Alder,[3] C.S. Amarasinghe,[4,*] A. Ames,[1,2] T.J. Anderson,[1,2] N. Angelides,[5] H.M. Araújo,[5] J.E. Armstrong,[6] M. Arthurs,[1,2] A. Baker,[5] S. Balashov,[7] J. Bang,[8] J.W. Bargemann,[9] A. Baxter,[10] K. Beattie,[11] T. Benson,[12] A. Bhatti,[6] A. Biekert,[11,13] T.P. Biesiadzinski,[1,2] H.J. Birch,[4] E. Bishop,[14] G.M. Blockinger,[15] B. Boxer,[16,†] C.A.J. Brew,[7] P. Brás,[17] S. Burdin,[10] M. Buuck,[1,2] M.C. Carmona-Benitez,[18] M. Carter,[10] A. Chawla,[19] H. Chen,[11] J.J. Cherwinka,[12] N.I. Chott,[20] M.V. Converse,[21] A. Cottle,[3] G. Cox,[22] D. Curran,[22] C.E. Dahl,[23,24] A. David,[3] J. Delgaudio,[22] S. Dey,[25] L. de Viveiros,[18] C. Ding,[8] J.E.Y. Dobson,[26] E. Druszkiewicz,[21] S.R. Eriksen,[27,‡] A. Fan,[1,2] N.M. Fearon,[25] S. Fiorucci,[11] H. Flaecher,[27] E.D. Fraser,[10] T.M.A. Fruth,[28] R.J. Gaitskell,[8] A. Geffre,[22] J. Genovesi,[20] C. Ghag,[3] R. Gibbons,[11,13] S. Gokhale,[29] J. Green,[25] M.G.D.van der Grinten,[7] C.R. Hall,[6] S. Han,[1,2] E. Hartigan-O'Connor,[8] S.J. Haselschwardt,[11] S.A. Hertel,[30] G. Heuermann,[4] G.J. Homenides,[31] M. Horn,[22] D.Q. Huang,[4] D. Hunt,[25] C.M. Ignarra,[1,2] E. Jacquet,[5] R.S. James,[3] J. Johnson,[16] A.C. Kaboth,[19] A.C. Kamaha,[32] D. Khaitan,[21] A. Khazov,[7] I. Khurana,[3] J. Kim,[9] J. Kingston,[16] R. Kirk,[8] D. Kodroff,[18] L. Korley,[4] E.V. Korolkova,[33] H. Kraus,[25] S. Kravitz,[11,34] L. Kreczko,[27] B. Krikler,[27] V.A. Kudryavtsev,[33] J. Lee,[35] D.S. Leonard,[35] K.T. Lesko,[11] C. Levy,[15] J. Lin,[11,13] A. Lindote,[17] R. Linehan,[1,2] W.H. Lippincott,[9] M.I. Lopes,[17] E. Lopez Asamar,[17] W. Lorenzon,[4] C. Lu,[8] S. Luitz,[1] P.A. Majewski,[7] A. Manalaysay,[11] R.L. Mannino,[36] C. Maupin,[22] M.E. McCarthy,[21] G. McDowell,[4] D.N. McKinsey,[11,13] J. McLaughlin,[23] R. McMonigle,[15] E.H. Miller,[1,2] E. Mizrachi,[6,36] A. Monte,[9] M.E. Monzani,[1,2,37] J.D. Morales Mendoza,[1,2] E. Morrison,[20] B.J. Mount,[38] M. Murdy,[30] A.St.J. Murphy,[14] A. Naylor,[33] C. Nedlik,[30] H.N. Nelson,[9] F. Neves,[17] A. Nguyen,[14] J.A. Nikoleyczik,[12] I. Olcina,[11,13] K.C. Oliver-Mallory,[5] J. Orpwood,[33] K.J. Palladino,[25] J. Palmer,[19] N.J. Pannifer,[27] N. Parveen,[15] S.J. Patton,[11] B. Penning,[4] G. Pereira,[17] E. Perry,[3] T. Pershing,[36] A. Piepke,[31] Y. Qie,[21] J. Reichenbacher,[20] C.A. Rhyne,[8] Q. Riffard,[11] G.R.C. Rischbieter,[4,5] H.S. Riyat,[14] R. Rosero,[29] T. Rushton,[33] D. Rynders,[22] D. Santone,[19] A.B.M.R. Sazzad,[31] R.W. Schnee,[20] S. Shaw,[14] T. Shutt,[1,2] J.J. Silk,[6] C. Silva,[17] G. Sinev,[20] R. Smith,[11,13] V.N. Solovov,[17] P. Sorensen,[11] J. Soria,[11,13] I. Stancu,[31] A. Stevens,[3,5] K. Stifter,[24] B. Suerfu,[11,13] T.J. Sumner,[5] M. Szydagis,[15] W.C. Taylor,[8] D.R. Tiedt,[22] M. Timalsina,[11,20] Z. Tong,[5] D.R. Tovey,[33] J. Tranter,[33] M. Trask,[9] M. Tripathi,[16] D.R. Tronstad,[20] W. Turner,[10] A. Vacheret,[5] A.C. Vaitkus,[8] V. Velan,[11] A. Wang,[1,2] J.J. Wang,[31] Y. Wang,[11,13] J.R. Watson,[11,13] R.C. Webb,[39] L. Weeldreyer,[31] T.J. Whitis,[9] M. Williams,[4] W.J. Wisniewski,[1] F.L.H. Wolfs,[21] S. Woodford,[10] D. Woodward,[11,18] C.J. Wright,[27] Q. Xia,[11] X. Xiang,[8,29] J. Xu,[36] M. Yeh,[29] and E.A. Zweig[32]

(LZ Collaboration)

[1]*SLAC National Accelerator Laboratory, Menlo Park, CA 94025-7015, USA*
[2]*Kavli Institute for Particle Astrophysics and Cosmology, Stanford University, Stanford, CA 94305-4085 USA*
[3]*University College London (UCL), Department of Physics and Astronomy, London WC1E 6BT, UK*
[4]*University of Michigan, Randall Laboratory of Physics, Ann Arbor, MI 48109-1040, USA*
[5]*Imperial College London, Physics Department, Blackett Laboratory, London SW7 2AZ, UK*
[6]*University of Maryland, Department of Physics, College Park, MD 20742-4111, USA*
[7]*STFC Rutherford Appleton Laboratory (RAL), Didcot, OX11 0QX, UK*
[8]*Brown University, Department of Physics, Providence, RI 02912-9037, USA*
[9]*University of California, Santa Barbara, Department of Physics, Santa Barbara, CA 93106-9530, USA*
[10]*University of Liverpool, Department of Physics, Liverpool L69 7ZE, UK*
[11]*Lawrence Berkeley National Laboratory (LBNL), Berkeley, CA 94720-8099, USA*
[12]*University of Wisconsin-Madison, Department of Physics, Madison, WI 53706-1390, USA*
[13]*University of California, Berkeley, Department of Physics, Berkeley, CA 94720-7300, USA*
[14]*University of Edinburgh, SUPA, School of Physics and Astronomy, Edinburgh EH9 3FD, UK*
[15]*University at Albany (SUNY), Department of Physics, Albany, NY 12222-0100, USA*

Accepted Paper

First constraints on WIMP-nucleon effective field theory couplings in an extended energy region from LUX-ZEPLIN

Phys. Rev. D

J. Aalbers et al.

Accepted 26 March 2024

UNIVERSITY OF MICHIGAN

UNIVERSITAS TURICENSIS MDCCCXXXIII

University of Zurich UZH

Thank you for your time! Questions?

DEPARTMENT OF ENERGY UNITED STATES OF AMERICA

UKRI Science and Technology Facilities Council

Sanford Underground Research Facility
South Dakota Science and Technology Authority

FCT Fundação para a Ciência e a Tecnologia
MINISTÉRIO DA EDUCAÇÃO E CIÊNCIA

ibs Institute for Basic Science

Backup Slides

Going Further: Operators in a Non-Relativistic Effective Field Theory

Phys. Rev. C 89, 065501 (2014)
JCAPO2 (2013)

- Spin Independent and Spin Dependent interactions rely on the assumption of a zero-momentum transfer. But what if there is some momentum dependency?
- Use an EFT where we treat the WIMP-nucleon elastic scattering as a four-field interaction

$$\mathcal{L}_{int} = \mathcal{O}\chi^{+}\chi^{-}N^{+}\mathrm{N}^{-}$$

- 4 Galilean-invariant, Hermitian quantities which describe the interaction

$$i\vec{q},\, \vec{S}_{\chi},\, \vec{S}_{N},\, \vec{v}^{\perp} \equiv \vec{v} + \frac{\vec{q}}{2\mu_N}$$

- Linear combinations up to second-order of momentum →15 operators which contribute to the interaction Lagrangian
- Differential Recoil Rate in this case

$$\frac{dR}{dE_R} = \frac{\rho_\chi}{32\,\pi m_\chi^3 m_N^2}\int_{v>v_{min}}^{\infty} \frac{f(\vec{v})}{v} \sum_{i,j=1}^{15} \sum_{a,b=0,1} c_j^a c_i^b F_{i,j}^{a,b} d^3 v$$

- This framework can also be mapped onto covariant Lagrangians, allowing for more complex interactions to be studied (coming in a future paper).

$$\begin{aligned}\mathcal{L}_{int} &= \sum_i c_i \mathcal{O}_i \\ &= c_1 + ic_3\vec{S}_N\cdot(\vec{q}\times\vec{v}^{\perp}) + c_4\vec{S}_\chi\cdot\vec{S}_N \\ &+ ic_5\vec{S}_\chi\cdot(\vec{q}\times\vec{v}^{\perp}) + c_6(\vec{S}_\chi\cdot\vec{q})(\vec{S}_N\cdot\vec{q}) \\ &+ c_7\vec{S}_N\cdot\vec{v}^{\perp} + c_8\vec{S}_\chi\cdot\vec{v}^{\perp} + ic_9\vec{S}_\chi\cdot(\vec{S}_N\times\vec{q}) \\ &+ c_{10}\vec{S}_N\cdot\vec{q} + ic_{11}\vec{S}_\chi\cdot\vec{q} + c_{12}\vec{S}_\chi\cdot(\vec{S}_N\times\vec{v}^{\perp}) \\ &+ ic_{13}(\vec{S}_\chi\cdot\vec{v}^{\perp})(\vec{S}_N\cdot\vec{q}) + ic_{14}(\vec{S}_\chi\cdot\vec{q})(\vec{S}_N\cdot\vec{v}^{\perp}) \\ &+ -c_{15}(\vec{S}_\chi\cdot\vec{q})\left((\vec{S}_N\times\vec{v}^{\perp})\cdot\vec{q}\right)\end{aligned}$$

Recoil Rates from NREFT Operators

- Simplest case: assume no interference between operators: $c_i c_j = 0$ for $i \neq j$
- Solid lines: Isoscalar couplings   Dashed lines: Isovector couplings
- Typical SI WIMP Search: 0-50 keV → Poor search window for NREFT Interactions!
- Shaded regions are where detection threshold falls below 50% after final data selection criteria

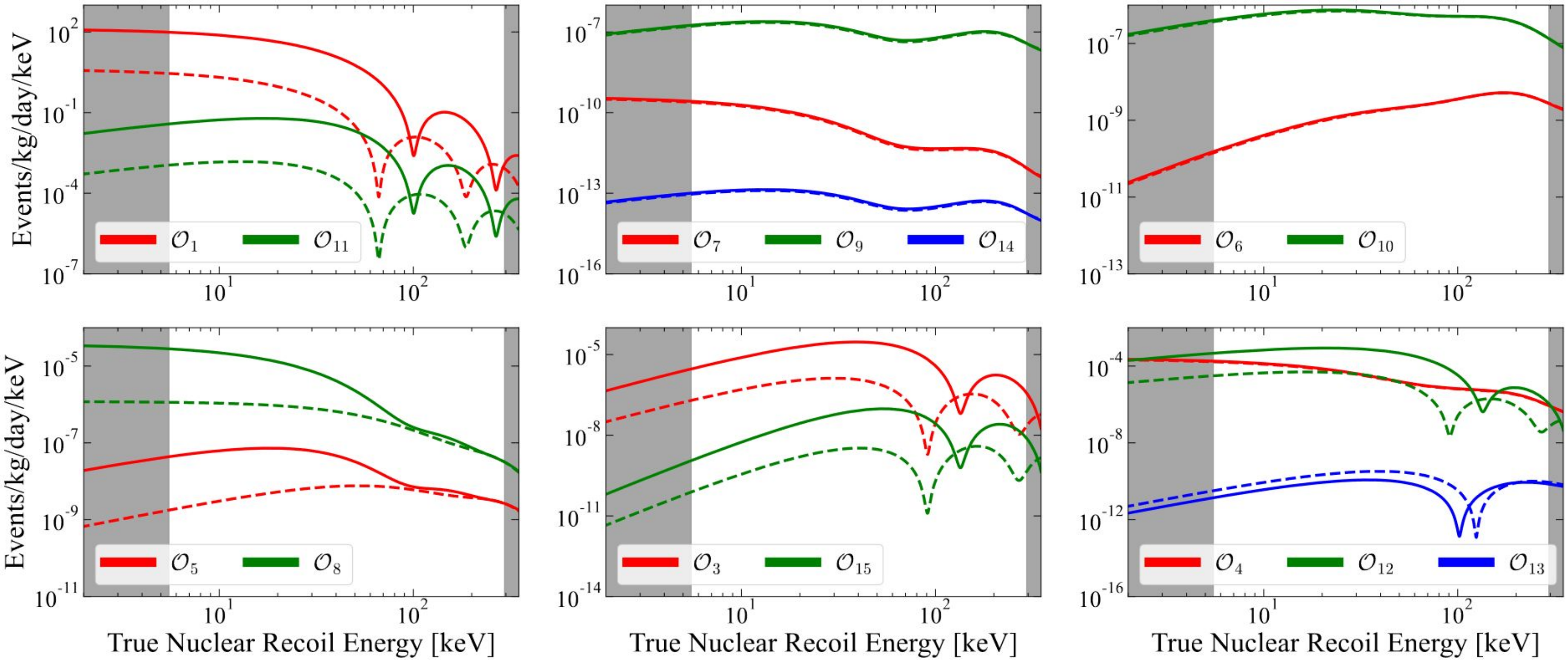

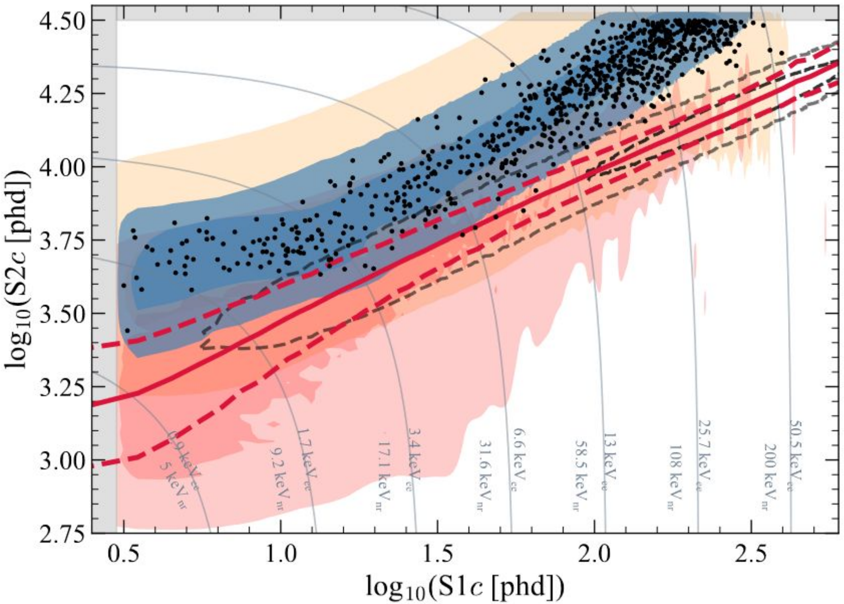

Source	Expected Events	Fit Result
Flat ER	517.4 ± 82.8	574.7 ± 30.2
Detector ER	18.4 ± 9.2	22.3 ± 8.1
ν ER	55.3 ± 5.5	55.5 ± 5.5
^{124}Xe	8.2 ± 2.0	8.7 ± 2.0
^{127}Xe	20.5 ± 1.8	20.8 ± 1.8
^{136}Xe	55.1 ± 11.6	58.2 ± 11.2
^{125}I	30.1 ± 15.6	34.2 ± 8.9
^{8}B CEνNS	0.14 ± 0.01	0.14 ± 0.01
Accidentals	1.3 ± 0.3	1.3 ± 0.03
Subtotal	706 ± 86	775 ± 34
^{37}Ar	[0, 288]	49.5 ± 9.4
Detector neutrons	$0.0^{+0.5}$	$0.0^{+1.8}$
Total	-	825 ± 36

Fit results

WIMP-like ER Pathologies: γ-X Events

- As the energy window increases, the observed rate of ER contributions from detector components increases
  - γ radiation: can multiply scatter in the target volume
- **γ-X Events**: Multiple S1-contributing scatters, one S2-contributing scatter
  - Custom simulation framework utilizing LZ geometry, field maps, and NEST response models to simulate γ propagation and yields for multiply-scattering events

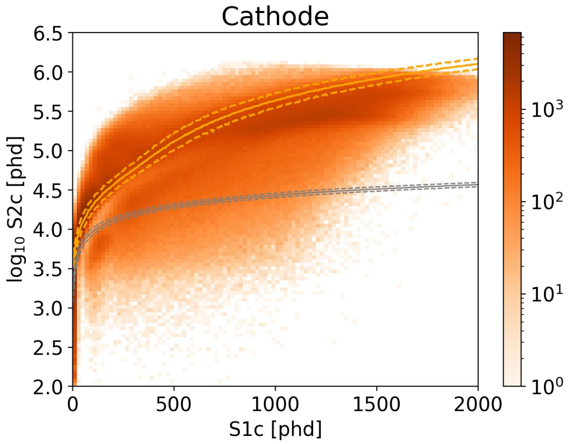

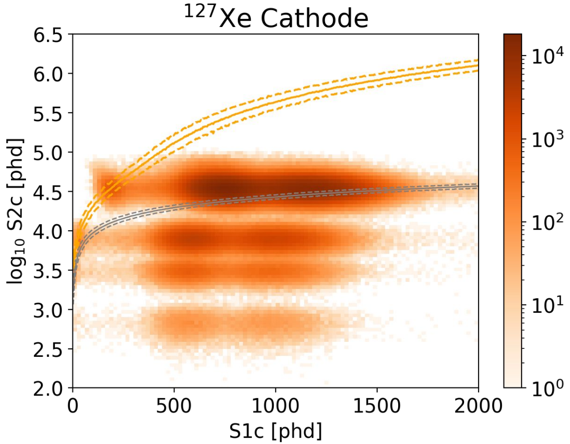

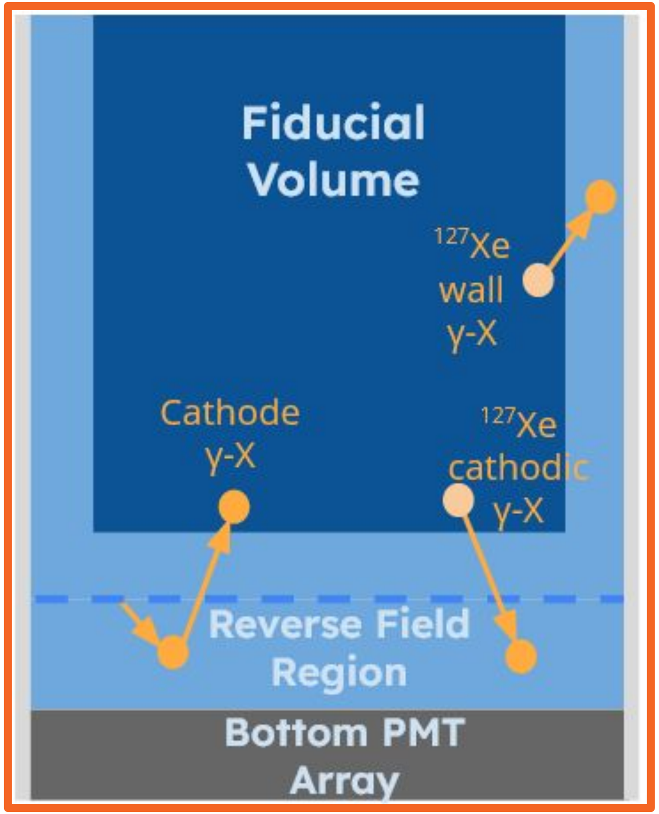

Removing γ-X Events: Boosted Decision Tree Classifier

- BDT trained on simulation data and tested on calibration data in a six-dimensional parameter space:
  - S1c, $\log_{10}$(S2c), Radial Position, Drift Time, *Cluster Size* (spread of hit pattern in the bottom PMT array), *Max Peak Area Fraction, Top-Bottom Asymmetry*
- WS sideband + simulation used to inform the rate in the EFT search window
  - Expected 1.6 ± 0.3 events → two were tagged and removed

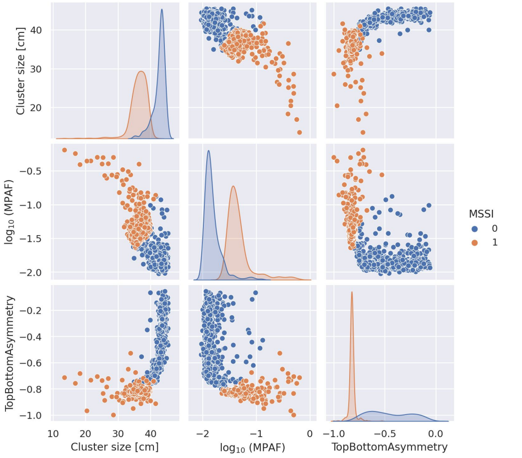

↓ P, → T	SS	γ-X
SS	99.997 ± 0.005	0.4 ± 1.2
γ-X	0.003 ± 0.005	99.6 ± 1.2

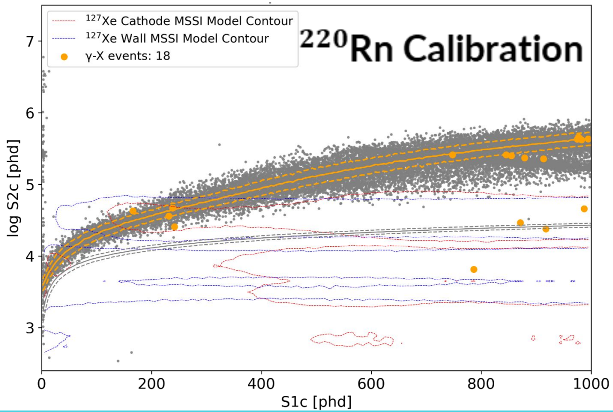

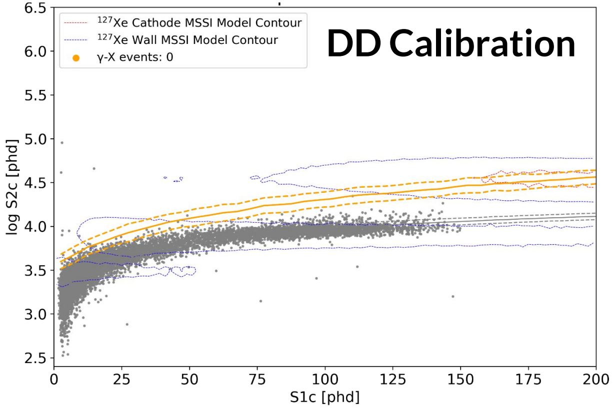

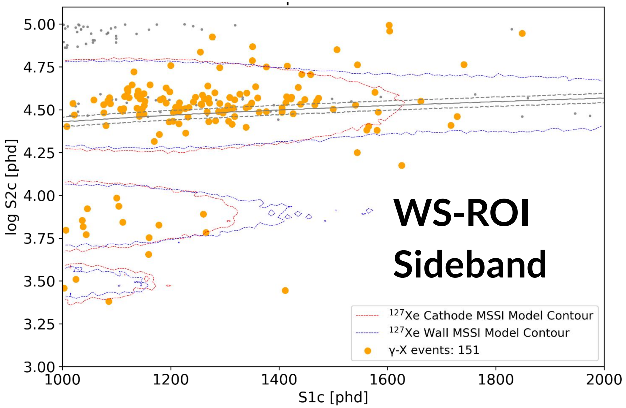

Benefit from an wider energy window

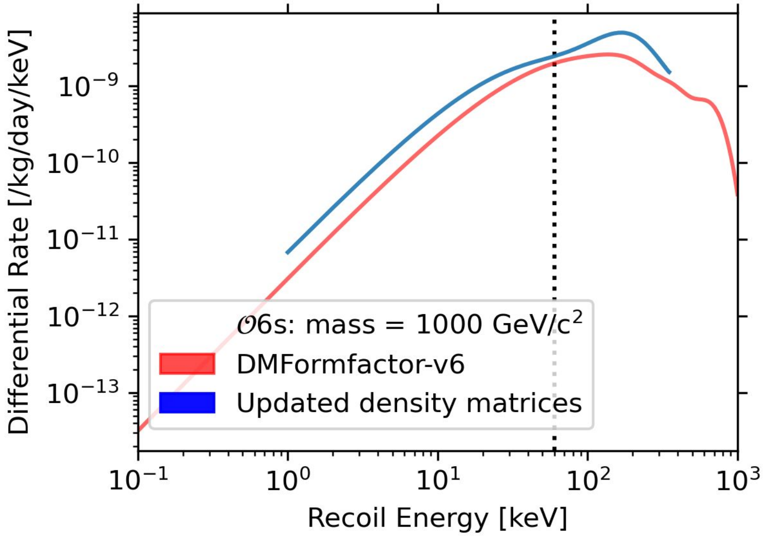

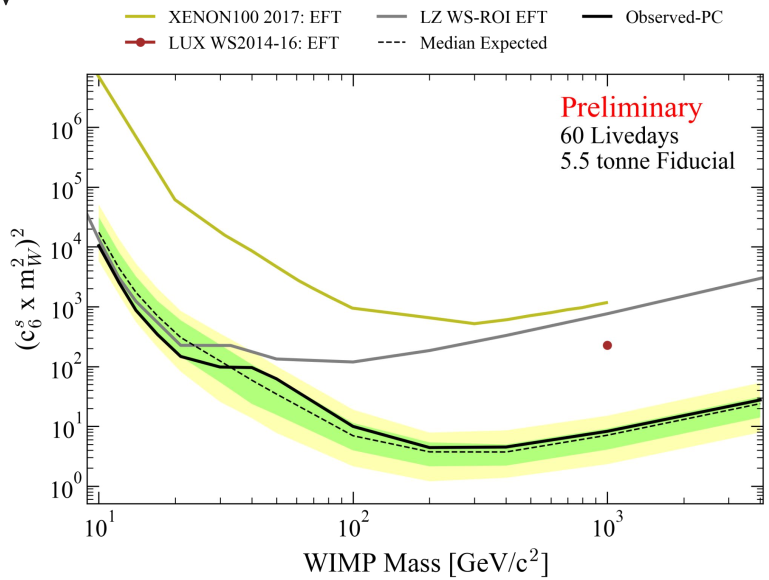

Dashed line indicates the energy at falling edge of the efficiency is 50% with LZ SR1 WIMP-Search ROI:

- $3 < S1_c[\text{phd}] < 80$

Grey:

- $3 < S1_c[\text{phd}] < 80$
- DMFormFactor-v6 signal

Black + Brazilian band (this work):

- $3 < S1_c[\text{phd}] < 600$, $\log_{10}(S2_c[\text{phd}]) < 4.5$
- Updated density matrices for signals

Impacts from updated nuclear density matrices

Differential recoils used updated GCN5082 ground state to ground state one-body density matrices

These have significant impacts on some operators

$\mathcal{O}_{13}$ differential rate has decreased significantly

$\mathcal{O}_{14}$ has the opposite behaviour

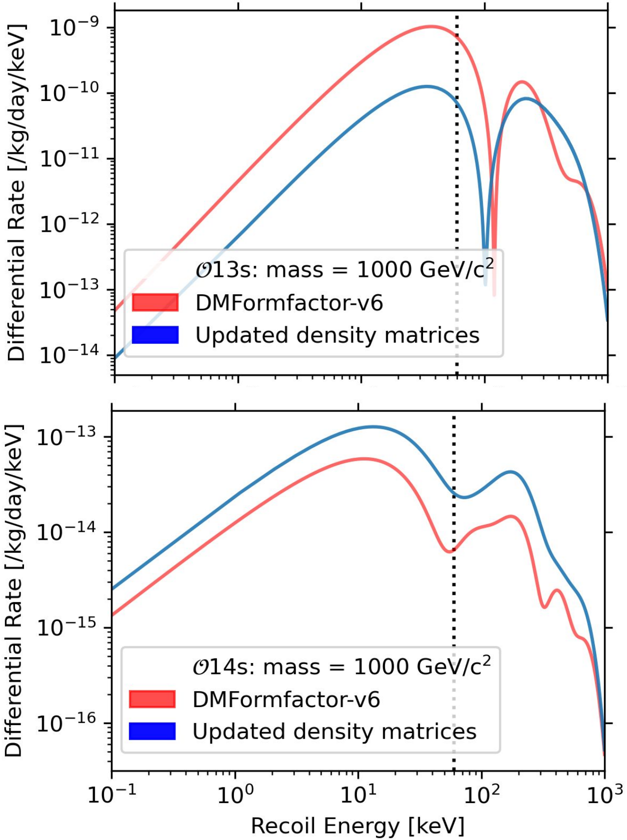

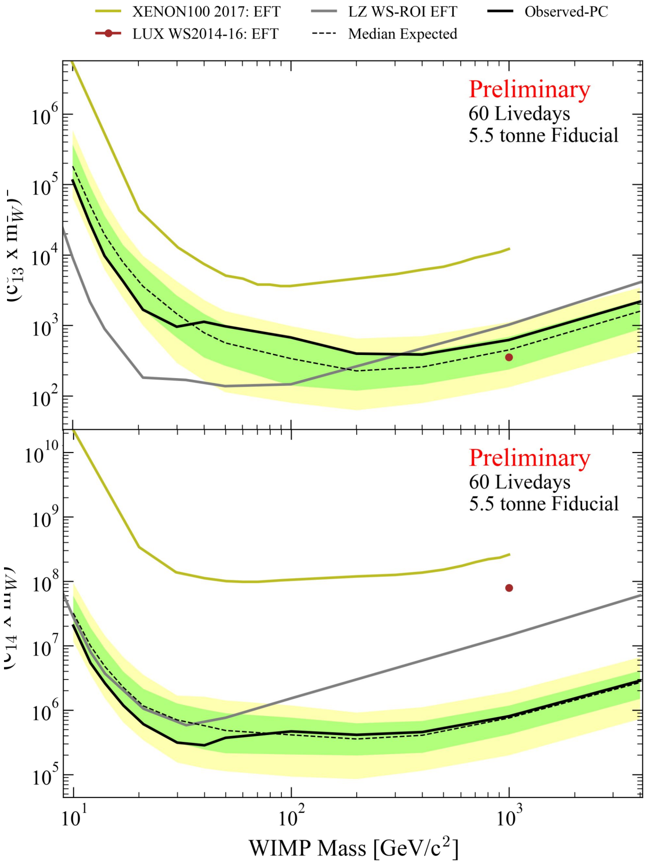

Signal PDFs in S1c,$\log_{10}$(S2c) space

Impact of ER leakage differs for various Operator models

ER leakage into the NR signal region primarily occurs between ~10-50 phd

Less impactful for WIMP models with a dominant contribution at higher energies

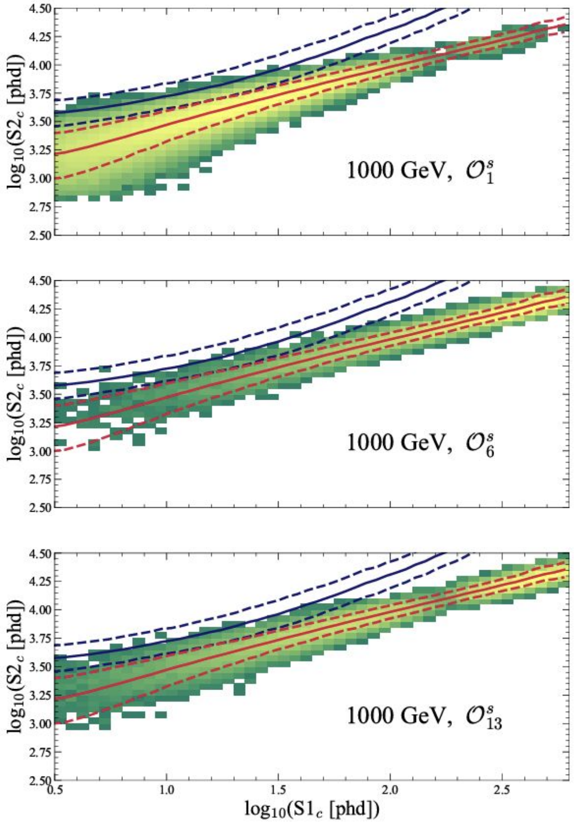

All 14 isoscalar limits from 10-4000 GeV/c^2

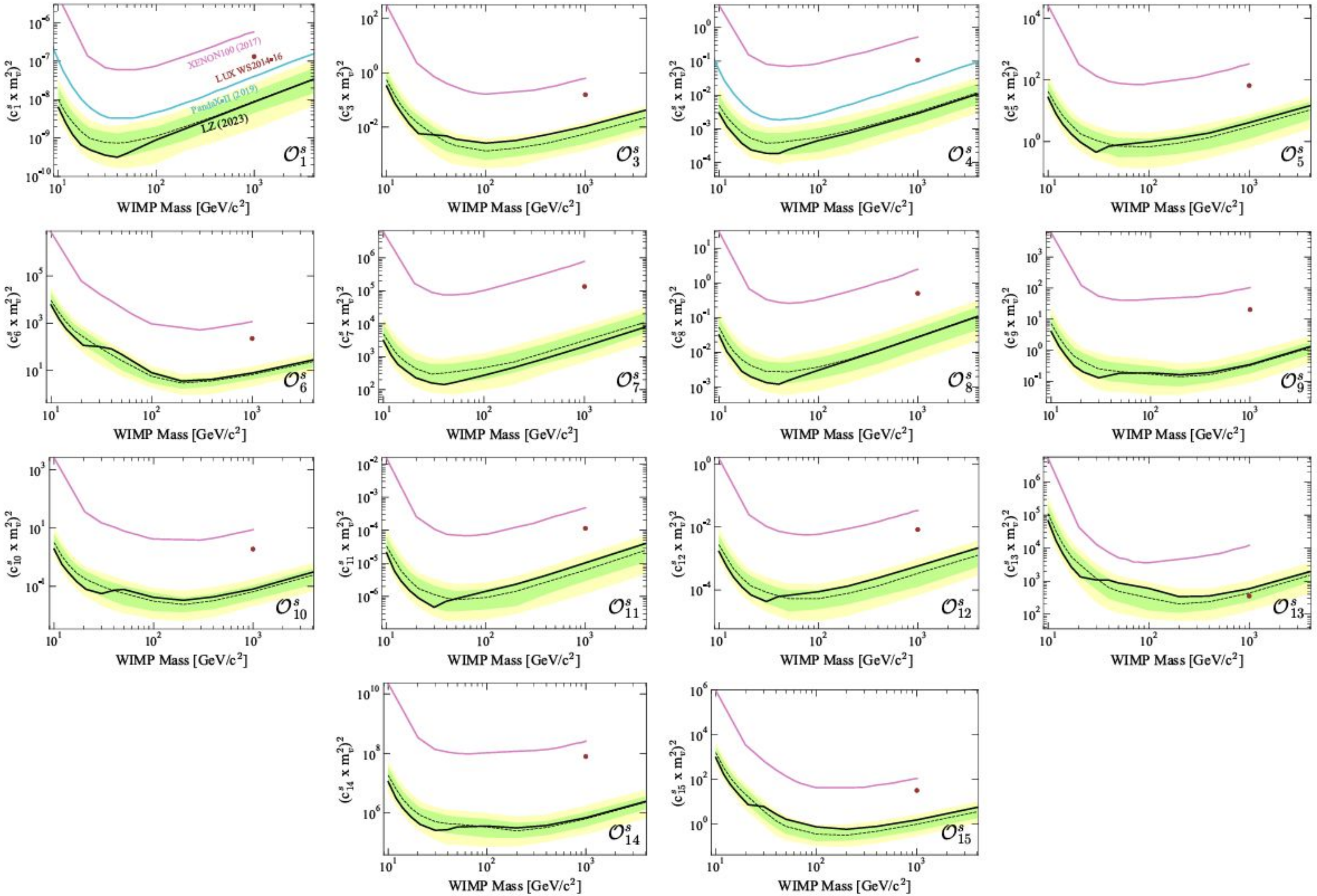

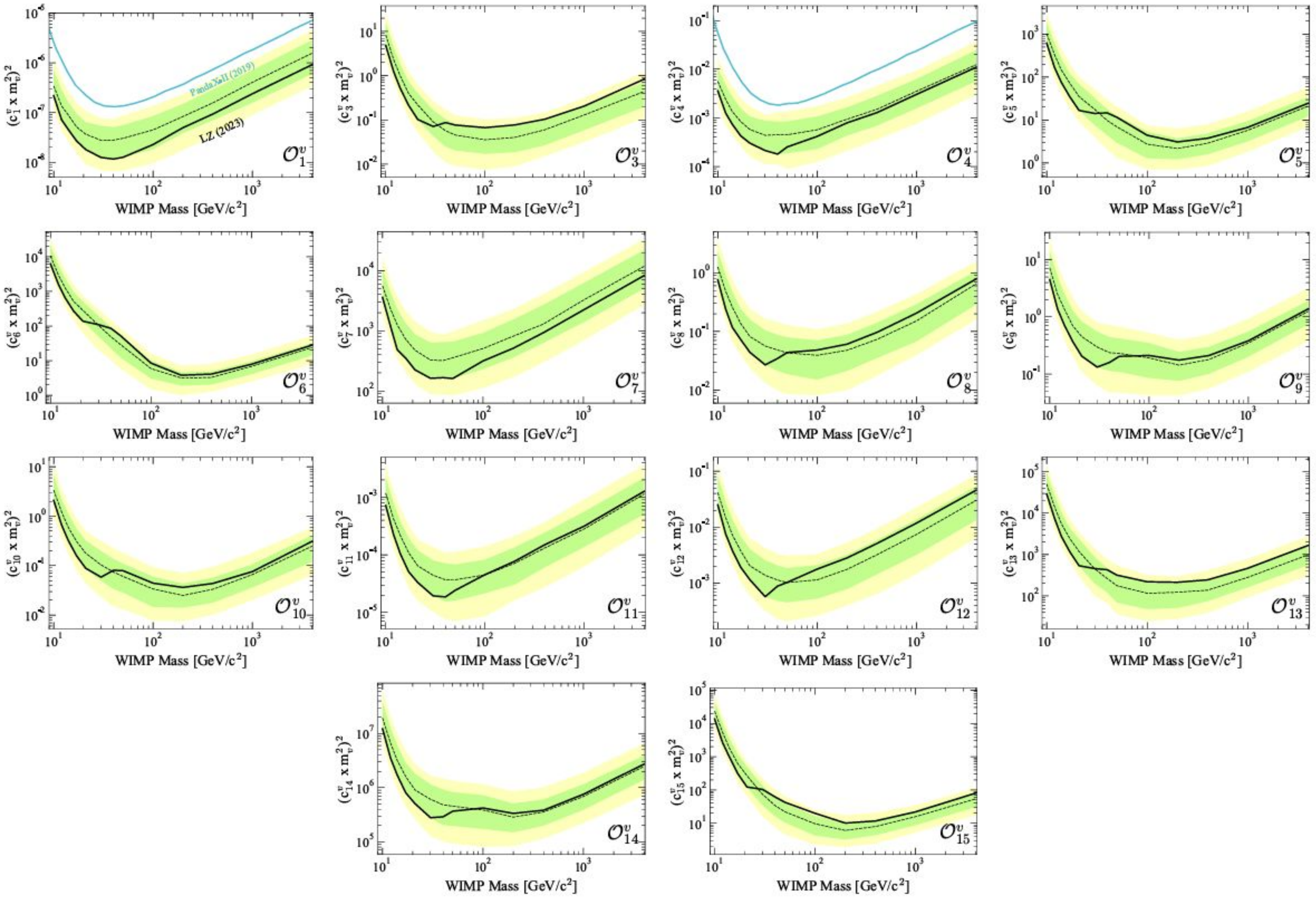

All 14 isovector limits from 10-4000 GeV/c^2

Equating Older Results: Dealing with differing conventions

TABLE III. LXe direct detection experiments that have reported SI and $\mathcal{O}_1^s$ limits. For NREFT limits, the isospin basis used is given for each experiment. The dimension in which the limit was reported is given for each as well as the conversion used to recast the limit in Fig. 11.

Experiment	Basis	Limit Type	Conversion in plot
Xenon100: 2017 NREFT [10]	$c^s = \frac{1}{2}(c^p + c^n)$ $c^v = \frac{1}{2}(c^p - c^n)$	$(c_i^s \times m_v^2)^2$	None
LUX: WS2014-16 NREFT [9]	$c^s = (c^p + c^n)$ $c^v = (c^p - c^n)$	$(c_i^s \times m_v^2)^2$	$\frac{1}{4}$
PandaX-II: SD EFT [8]	$c^s = \frac{1}{2}(c^p + c^n)$ $c^v = \frac{1}{2}(c^p - c^n)$	$d_5^{s/v}$ $[\frac{1}{m_v^2}]$	$(d_5^s)^2$
LZ NREFT (This analysis)	$c^s = \frac{1}{2}(c^p + c^n)$ $c^v = \frac{1}{2}(c^p - c^n)$	$(c_i^{s/v} \times m_v^2)^2$	None
NRET Theory paper [14]	$c^s = \frac{1}{2}(c^p + c^n)$ $c^v = \frac{1}{2}(c^p - c^n)$	N/A	N/A
LUX: Combined 2017 SI [55]	N/A	σ_{SI}^N	$\sigma_{SI}^N \frac{\pi \cdot m_v^4}{(\frac{(\hbar c)}{\text{GeV}})^2 \mu_N^2}$
PandaX-4T: 2021 SI [56]	N/A	σ_{SI}^N	$\sigma_{SI}^N \frac{\pi \cdot m_v^4}{(\frac{(\hbar c)}{\text{GeV}})^2 \mu_N^2}$
LZ: 2023 SI [1]	N/A	σ_{SI}^N	$\sigma_{SI}^N \frac{\pi \cdot m_v^4}{(\frac{(\hbar c)}{\text{GeV}})^2 \mu_N^2}$
XENONnT: 2023 SI [2]	N/A	σ_{SI}^N	$\sigma_{SI}^N \frac{\pi \cdot m_v^4}{(\frac{(\hbar c)}{\text{GeV}})^2 \mu_N^2}$